Nature of weak inter- and intramolecular contacts in crystals
2. Character of electron delocalization and the nature of X—H...H—X (X = C, B) contacts in the crystal of 1-phenyl-*o*-carborane

I. V. Glukhov,[a,b] K. A. Lyssenko,[a] A. A. Korlyukov,[a] and M. Yu. Antipin[a]*

[a]*A. N. Nesmeyanov Institute of Organoelement Compounds, Russian Academy of Sciences, 28 ul. Vavilova, 119991 Moscow, Russian Federation. Fax: +7 (095) 135 5085. E-mail: kostya@xray.ineos.ac.ru*
[b]*Higher Chemical College, Russian Academy of Sciences, 9 Miusskaya pl., 125820 Moscow, Russian Federation*

High-resolution single-crystal X-ray study of 1-phenyl-*o*-carborane was carried out and the experimental and theoretical (B3LYP/6-311G** calculated) electron density distributions in the title compound were investigated. Character of electron delocalization in 1-phenyl-*o*-carborane was examined by analyzing the deformation electron density maps, maps of the Laplacian of the electron density, and maps of the electron localization function. Crystal-structure-forming X—H...H—X (X = C, B) intermolecular contacts were revealed and analyzed. The energies and geometric parameters of these contacts were compared with the results of quantum-chemical calculations of the crystal structure and with characteristics of the same type of intramolecular contacts.

Key words: organic carborane derivatives, C—H...H—B and B—H...H—B contacts, supramolecular chemistry, electron density distribution, topological theory "Atoms in molecules", X-ray diffraction data, quantum-chemical calculations.

Recently, studies on the nature of weak intramolecular and intermolecular contacts have been the subject of considerable attention in structural chemistry of carboranes, along with investigations on features of the molecular structure and search for "structure—reactivity" relationships.[2—5] The carborane structures are comprised of C and B atoms bonded to positively and negatively charged hydrogens, respectively. This makes it possible to form a variety of intermolecular contacts of different nature. For instance, a number of cyclotriveratrilene-based inclusion compounds containing an unsubstituted icosahedral *o*-carborane were obtained,[2—4] the structure of this carborane being analyzed for the first time.[2] The main types of the intermolecular contacts responsible for molecular recognition processes in these inclusion compounds are the C—H...O and C—H...π contacts. A study[5] of a co-crystal of diaza-18-crown-6 with *o*-carborane revealed not only C—H...O but also B—H...H—N contacts.

As to substituted carboranes, the C—H...O, C—H...N, and C—H...F interactions were also reported (see Ref. 6). Considering unsubstituted carboranes or carboranes whose atoms are usually not involved in specific interactions, we can assume that the main type of structure-forming contacts are $B—H^{\delta-}...H^{\delta+}—C_{carb}$ contacts. Taking into account the fact that the shortened H...H distance cannot serve as a sufficient criterion for an intermolecular contact, it was interesting to perform a high-resolution X-ray diffraction study of the electron density distribution in the crystal of such compound. Since unsubstituted carboranes form plastic crystals in a wide temperature range[7] and therefore obtaining of single crystals presents a very complicated problem, in this work we carried out a single-crystal study of 1-phenyl-*o*-carborane (**1**, Fig. 1).

Additional interest in compound **1** is due to the presence of forced H...H intramolecular contacts in the molecule at any conformation of the phenyl ring.[8] A recent study of the electron density distribution in isolated molecule **1** revealed an attractive character of these interactions.[9] Hence we can compare (i) this type of intramolecular and intermolecular interactions and (ii) experimental data and results of calculations in order to assess the applicability of X-ray diffraction studies of the electron density distribution (ρ(**r**) function) in the investigations of so weak interactions.

* For Part 1, see Ref. 1.

Published in Russian in *Izvestiya Akademii Nauk. Seriya Khimicheskaya,* No. 3, pp. 541—552, March, 2005.

1066-5285/05/5403-0547

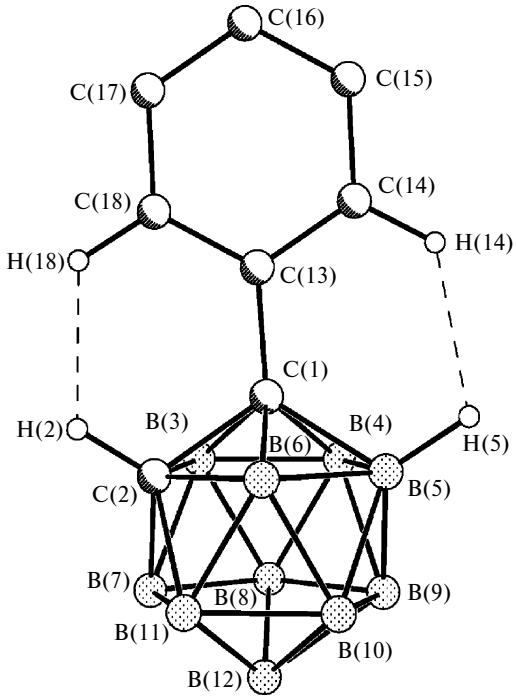

Fig. 1. Overall view of the molecule of compound **1**. Shown are only those hydrogen atoms that form intramolecular H...H contacts.

Results and Discussion

Molecular and crystal structure

The structure of 1-phenyl-*o*-carborane has been studied in detail in the crystal, in solution, and in the gas phase.[8–11] An X-ray diffraction study[8] revealed two polymorphs, α-**1** and β-**1**, containing two and one independent molecule in the unit cell, respectively. The unsubstituted C atom in one out of two α-**1** molecules is equiprobably disordered over the pentagonal face.[8] Therefore, in this work we studied the ordered[12] modification, β-**1**.

The main bond lengths in molecule **1** at 110 K coincide with those determined[12] at 150 K. The ordered molecules of the α-**1** and β-**1** polymorphs are characterized by nearly identical mutual arrangement of the phenyl ring and icosahedron. For instance, the C(2)—C(1)—C(13)—C(14) (θ) torsion angle is 18.6 for α-**1** and 22.3° for β-**1**. This leads to formation of shortened contacts, H(2)...H(18) and H(5)...H(14), of length 2.041 and 2.148 Å, respectively (see Fig. 1).

Studies[8,9,11] of molecule **1** in the gas phase and in solution showed that although the conformation of the molecule in the crystal is stable, the barrier to rotation about the C(1)—C(13) bond is very low (B3LYP/6-31G** calculations[9] gave 0.3 kcal mol^{-1}, which is consistent with the results of gas-phase electron diffraction study). The minimum energy was obtained at θ = 30.2° (B3LYP/6-31G** calculations[9]) and 36° (gas-phase electron diffraction study[8]).

Therefore, shortened H...H intramolecular contacts between hydrogens bonded to the carborane cage and to the phenyl ring carbons as well as the C(2)—H(2)...H(18)—C(18) contact (at θ = 0°) cause no increase in the barrier to rotation.[9]

It should be noted that the C(1)—C(2) bond length in molecule **1** is considerably different from the corresponding bond length in unsubstituted *o*-carborane (1.620 Å) and in some mono-substituted carborane derivatives with aryl ligands. Analysis of the data retrieved from the Cambridge Structural Database (CSD)[13] showed that the C(1)—C(2) bond lengths in nine available ordered structures ($R < 10\%$) of monoaryl *ortho*-carborane derivatives varies between 1.633 and 1.676 Å, being the largest at θ ≈ 90°.[9] This was explained in recent theoretical studies of compound **1**.[8–11] A quantum-chemical scan of the potential energy surface (PES) along the coordinate correspoding to the torsion angle θ revealed that although the barrier to rotation of the phenyl ring in molecule **1** is low, the C(1)—C(2) bond length varies from 1.641 to 1.672 Å, the remaining structural parameters of the molecule being independent of the θ value. Based on the results of the topological analysis of the ρ(**r**) function according to Bader[14,15] and taking into account that the C(1)—C(2) bond length is maximum at θ = 90°, it was shown[9–11] that elongation of this bond is due to transfer of the π-electron density of the phenyl ring to the antibonding orbital of the C(1)—C(2) bond.

Analysis of the crystal packing showed that each molecule in the crystal of the β-**1** polymorph has a total of eleven neighbors. The lengths of the intermolecular contacts vary over a rather wide range from 2.28 to 2.60 Å. The C—H...H—B contacts of average length 2.35 Å are systematically shorter than the B—H...H—B contacts (2.51 Å), most of which are longer than the sum of the van der Waals radii of two hydrogen atoms (Table 1, Fig. 2). The shortest contact, C—H...H—B, involves the H(2) atom bonded to the carbon atom of the carborane icosahedron; this is consistent with high acidity of the H(2) atom compared to the phenyl ring hydrogens.[7] The shortest intermolecular contact is much longer than intramolecular H...H contacts (2.04—2.15 Å).

It should be noted that in the crystal of the α-**1** polymorph the C(2)—H(2)...H—B contact was observed[8] only for the ordered molecule (H...H 2.34 Å). Based on this fact, we can assume that it is the absence of similar contacts in the second independent molecule of the α-**1** polymorph that is responsible for the observed disorder of the C atom.

In order to understand which intermolecular and intramolecular H...H contacts in the molecule of the β-**1** poly-

Table 1. Parameters of intermolecular H...H contacts obtained from X-ray diffraction study of the crystal of compond **1** and from DFT (PBE) calculations of molecule **1**

Contact	Experiment				Calculations			
	ST[a]	$d_{H...H}$/Å	Angle/deg		ST[a]	$d_{H...H}$/Å	Angle/deg	
			X—H...H	X...H—X			X—H...H	X...H—X
C(2)—H(2)...H(7′)—B(7′)[b]	3655 3645	2.280	156.4	104.8	3655 3645	2.614	147.4	110.2
C(2)—H(2)...H(12′)—B(12′)	3655 3645	2.578	111.5	101.7	—	—	—	—
B(3)—H(3)...H(8′)—B(8′)	—	—	—	—	3555 3545	2.241	166.6	155.7
B(3)—H(3)...H(11′)—B(11′)	1455 1655	2.583	115.6	145.3	—	—	—	—
B(3)—H(3)...H(17′)—C(17′)	3545 3555	2.427	128.3	124.7	3545 3555	2.423	116.2	120.0
B(3)—H(3)...H(18′)—C(18′)	—	—	—	—	3545 3555	2.513	113.5	117.2
B(4)—H(4)...H(10′)—B(10′)	1455 1655	2.491	158.9	109.1	—	—	—	—
B(5)—H(5)...H(10′)—B(10′)	2655 2655	2.519	108.7	172.8	2655 2655	2.191	113.4	174.7
B(6)—H(6)...H(15′)—C(15′)	2565 2565	2.327	150.6	127.7	—	—	—	—
B(7)—H(7)...H(12′)—B(12′)	3655 3645	2.450	112.4	117.1	3655 3645	2.365	122.4	129.0
B(8)—H(8)...H(11′)—B(11′)	3645 3655	2.430	139.2	120.8	—	—	—	—
B(9)—H(9)...H(14′)—C(14′)	2555 2555	2.411	114.8	118.1	—	—	—	—
B(9)—H(9)...H(15′)—C(15′)	2555 2555	2.360	160.1	120.5	2555 2555	2.387	157.9	132.6
B(10)—H(10).....H(10′)—B(10′)	2655	2.601	109.7	109.7				
B(12)—H(12)...H(17′)—C(17′)	1645 1465	2.323	146.5	130.0	1645 1465	2.254	152.0	128.5

[a] Symmetry transformations, where 3655 = $1 - x$, $0.5 + y$, $0.5 - z$; 3645 = $1 - x$, $-0.5 + y$, $0.5 - z$; 1455 = $-1 + x$, y, z; 1655 = $1 + x$, y, z; 2655 = $1 - x$, $-y$, $-z$; 2565 = $-x$, $1 - y$, $-z$; 2555 = $-x$, $-y$, $-z$; 1645 = $1 + x$, $-1 + y$, z; 1465 = $-1 + x$, $1 + y$, z; 3545= $-x$, $-0.5 + y$, $0.5 - z$; and 3555 = $-x$, $0.5 + y$, $0.5 - z$.

[b] The C—H and B—H distances were normalized to the "ideal" values obtained from quantum-chemical calculations (1.08 and 1.20 Å, respectively).

morph correspond to attractive interactions, we performed a topological analysis of the electron density distribution in the crystal.

Analysis of the electron density distribution

Deformation electron density. The topological analysis of the electron density distribution ($\rho(\mathbf{r})$ function) in icosahedral carboranes is limited to experimental studies of 9-azido-*m*-carborane[16] and 8,9,10,12-tetrafluoro-*o*-carborane (**2**).[17] Besides, the *closo*-borane anions $B_6H_6^{2-}$, $B_7H_7^{2-}$, and $B_{12}H_{12}^{2-}$; *nido*-boranes B_2H_6, B_5H_9, and B_6H_{10}; *arachno*-borane B_4H_{10}; *p-closo*-carboranes $C_2B_3H_5$ and $C_2B_4H_6$ [18] were investigated theoretically and 1,5-dicarba-*closo*-pentaborane was studied experimentally.[19]

Investigations[16—19] showed that stabilization of carboranes and boranes is due to both concentration of electrons along the bond path and electron delocalization over trigonal faces of the polyhedron.

Earlier,[17] a study of compound **2** (the one and only *o*-carborane derivative studied at that time) revealed a substantial depletion of the electron density in the region of the C—C bond. This was substantiated by not only the deformation electron density (DED) maps but also by the maps of the Laplacian of the electron density, $\nabla^2\rho(\mathbf{r})$. Such a character of the distribution of the $\nabla^2\rho(\mathbf{r})$ values indicates an intermediate type of the interatomic interaction, being atypical of homopolar bonds. In the early

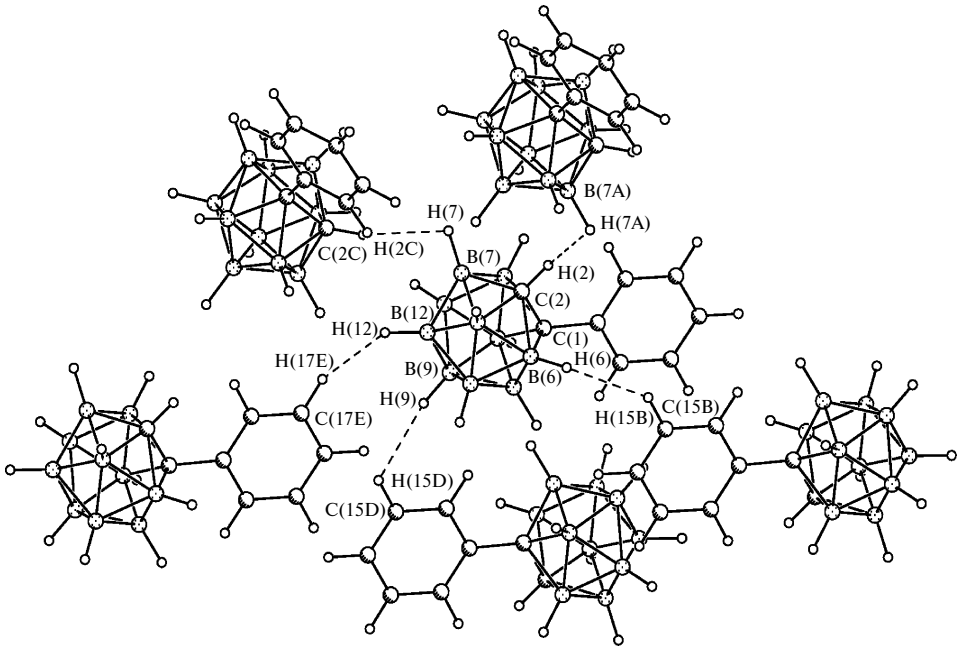

Fig. 2. Crystal packing fragment of the β-**1** polymorph, illustrating the formation of H...H contacts. Shown are only those molecules that form the H...H contacts of length at most 2.40 Å.

studies this was observed only for metal—metal bonds,[20] the O—O bonds in the H_2O_2 and hydroperoxide molecules, and for the F—F bond in the F_2 molecule.[21]

An intermediate character of the C—C bond in *o*-carborane is consistent with the fact that its length varies over a rather wide range compared to the C—B and B—B bonds in the icosahedron.[22] A feature of metallacarboranes containing bulky substituents at carbon atoms is formation (in some cases) of pseudo-*closo*-carborane structures with broken carbon—carbon bonds (with C(1)—C(2) distances longer than 2.0 Å).[22]

Since the intermediate type of interatomic interaction in compound **2** can be due to the electron-acceptor properties of fluorine atoms, it was interesting to assess the extent to which this type of interaction is typical of the C—C bond in *o*-carboranes.

The main features of the DED distribution in compound **1** are similar to those reported earlier for the derivative **2**.[17] Probably, the absence of electron-acceptor substituents at boron atoms leads to systematically higher positive values of the DED in the regions of the B—C, C—C, and B—B bonds. The section of the DED in the plane passing through the C(1), C(2), B(9), and B(12) atoms, the center of the carborane, and the phenyl substituent shows a depletion of the DED in the interior of the icosahedron and concentration (positive values) of the DED on the carborane surface (Fig. 3) Considerable electron delocalization over the surface of the polyhedron leads to a marked decrease in the positive DED values in the regions of the carborane C—B and B—B bonds compared to the regions of terminal C—H and B—H bonds and of C—C bonds in the phenyl ring.

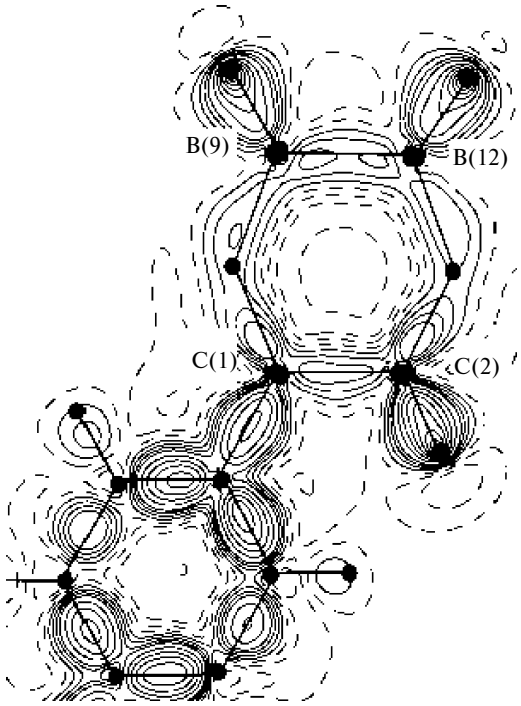

Fig. 3. Section of the DED in the plane passing through the C(1), C(2), B(9), and B(12) atoms.

In contrast to pentagonal faces, no clearly seen concentration of the DED in the bond path regions was found

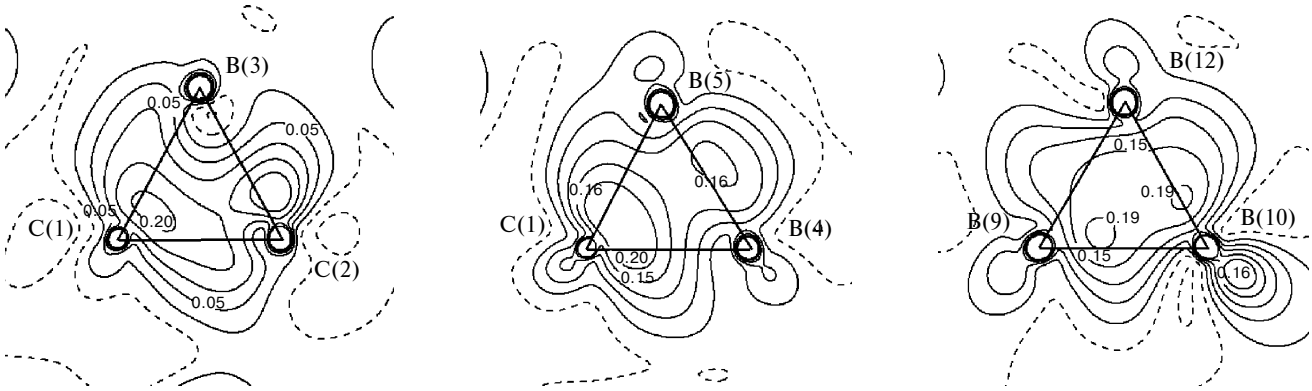

A B C

Fig. 4. DED distribution maps for the C(1)—C(2)—B(3) (**A**), C(1)—B(4)—B(5) (**B**), and B(9)—B(10)—B(12) (**C**) faces.

for the triangular faces of the icosahedron. Depending on the type of the atoms arranged on the face, the character of the DED distribution varies to some extent (Fig. 4). Maxima of the DED on the CCB and CBB faces are shifted toward carbon atoms due to different electronegativities of the atoms. For instance, a DED maximum of 0.2 e • Å^{-3} on the C(1)—B(4)—B(5) triangular face is shifted toward the C(1) atom and lies on the bisectrix of the B—C—B angle, whereas the DED maximum in the B—B line is at most 0.15 e • Å^{-3}. In the case of inequivalent boron atoms the peak is shifted toward that boron atom that is more affected by the electron-acceptor carbon atoms. For instance, the DED peak in the B—B line on the C(2)—B(6)—B(11) face is shifted toward the B(6) atom that is additionally bonded to the C(1) atom.

Concentration of the DED in the regions of triangular BBB faces is characterized by a more uniform distribution of positive DED values over the faces. Displacements of the DED maxima found in some cases are consistent with inequivalence of the boron atoms.

Thus, analysis of the DED distribution in molecule **1** unambiguously indicates that we can hardly distinguish between the concentration of electron density in the regions of the bond paths and on triangular faces, which points to considerable electron delocalization over the surface of the icosahedron.

Since the DED maps provide only qualitative information on the features of electron density distribution, we carried out a topological analysis of the ρ(**r**) function in the crystal of compound **1**. For comparison, we also performed a topological analysis of the electron density distribution function in isolated molecule **1** in the framework of B3LYP/6-311G** calculations.

Topological analysis of the ρ(r) function. The computational method employed in our calculations excellently reproduces the experimental geometry of molecule **1**. Earlier,[9] it was found that the topological characteristics of the C—B and C—C bonds vary depending on the conformation of the phenyl substituent. Therefore, in order to correctly compare the results of calculations and the experimental data, the geometry of molecule **1** was optimized with the θ angle set to 18.7°.

Good agreement between the dipole moment of the molecule in the crystal and in the gas phase (5.0 and 5.24 D, respectively) should also be pointed out. This allows one to hope for correct reproduction of subtle electronic effects in molecule **1**. For comparison, the dipole moment of the unsubstituted *o*-carborane molecule is 4.27 D.[11] Thus, introduction of phenyl substituent causes no charge redistribution, the increase in the dipole moment being due to an increase in linear diimensions of molecule **1**.

The theoretical and experimental ρ(**r**) functions have the same characteristic sets of critical points. They include the (3,−1) critical points in the regions of all chemical bonds, that is, B—B, C_{carb}—B, C_{carb}—C_{carb}, C_{phenyl}—C_{carb}, C_{phenyl}—H, C_{carb}—H, and B—H. In accordance with the Poincaré—Hopf relation,[14] a total of twenty-one (3,+1) ring critical points corresponding to twenty three-membered rings in the carborane cage and one six-membered ring (phenyl ring) and one (3,+3) critical point at the center of the icosahedron were found.

In addition to the expected critical points, the topological analysis of both theoretical and experimental ρ(**r**) functions revealed the (3,−1) critical points in the regions of the H(2)...H(18) and H(5)...H(14) intramolecular contacts which close the six-membered rings. Consequently, we found two additional ring critical points of the (3,+1) type. The H(2)...H(18) and H(5)...H(14) distances between the contacting atoms differ insignificantly, being respectively equal to 2.041 and 2.148 Å (experiment) and 2.086 and 2.166 Å (calculations).

The ρ(**r**) values at the (3,−1) critical points of the bonds in the polyhedron vary within a rather narrow interval, 0.74—1.25 e • Å^{-3} for the crystal and 0.81—1.22 e • Å^{-3} for isolated molecule **1**. In both cases the ρ(**r**) value is

maximum for the C(1)—C(2) bond and minimum for the B(7)—B(11) bond. The $\rho(\mathbf{r})$ values at the (3,−1) critical points, obtained for the bonds in the polyhedron are much smaller than the corresponding parameters of C—C bonds in the phenyl substituent and of terminal C—H bonds (Table 2).

It should be noted that the (3,−1) critical points in the region of the C—B bonds are markedly shifted from the midpoints of corresponding bonds toward boron atoms, which indicates that we are concerned with polar bonds.[14] The (3,−1) critical points of the C—B bonds in the crystal and in isolated molecule **1** are displaced to nearly the same extent, by 0.28 and 0.26 Å, respectively. For comparison, the (3,−1) critical point in the region of the C(1)—C(2) bond is at the midpoint of the bond while the (3,−1) critical point of the C(1)—C(13) bond is shifted toward the C(13) atom by 0.034 Å (calculations) and 0.01 Å (experiment). The last-mentioned values for the C(1)—C(2) and C(1)—C(13) bonds and the magnitude of the dipole moment of the molecule show that the electron density transfer from the phenyl ring to carborane is insignificant.

The experimental and theoretical values of the $\rho(\mathbf{r})$ function at the (3,−1) critical points of the bonds con-

Table 2. Topological parameters of the $\rho(\mathbf{r})$ function at the (3,−1) critical points in the crystal (multipole refinement) and in isolated molecule **1** (obtained from B3LYP/6-311G** calculations)

Bond	Crystal			Isolated molecule			Difference[a]		
	$\rho(\mathbf{r})$/e·Å^{-3}	$\nabla^2\rho(\mathbf{r})$/e·Å^{-5}	ε^b	$\rho(\mathbf{r})$/e·Å^{-3}	$\nabla^2\rho(\mathbf{r})$/e·Å^{-5}	ε	$\rho(\mathbf{r})$/e·Å^{-3}	$\nabla^2\rho(\mathbf{r})$/e·Å^{-5}	ε
C(1)—C(2)	1.23	−0.58	0.98	1.22	−4.34	0.80	0.01	3.76	0.18
C(1)—C(13)	1.76	−12.10	0.09	1.70	−14.07	0.05	0.06	1.98	0.04
C(1)—B(3)	0.88	−2.49	1.97	0.81	−1.93	3.43	0.07	0.56	1.46
C(1)—B(4)	0.86	−1.44	7.00	0.81	2.65	2.78	0.05	4.09	4.22
C(1)—B(5)	0.90	−3.31	4.23	0.81	2.89	2.97	0.09	6.21	1.26
C(1)—B(6)	0.80	−2.09	8.77	0.81	−1.69	3.40	0.01	0.41	5.37
C(2)—B(3)	0.80	−2.40	2.68	0.81	−0.48	3.33	0.01	1.92	0.65
C(2)—B(6)	0.93	−3.67	1.69	0.81	−0.96	3.60	0.12	2.71	1.91
C(2)—B(7)	0.92	−3.37	2.34	0.81	3.62	2.65	0.11	6.99	0.31
C(2)—B(11)	0.88	−3.39	2.95	0.81	3.62	2.61	0.07	7.01	0.34
C(13)—C(14)	2.26	−21.32	0.19	2.09	−20.00	0.22	0.16	1.32	0.03
C(13)—C(18)	2.19	−19.99	0.24	2.09	−19.76	0.22	0.10	0.23	0.02
C(14)—C(15)	2.22	−20.92	0.17	2.09	−20.73	0.21	0.12	0.20	0.04
C(15)—C(16)	2.25	−20.80	0.16	2.09	−20.74	0.21	0.16	0.06	0.05
C(16)—C(17)	2.26	−20.96	0.17	2.12	−20.74	0.21	0.14	0.22	0.04
C(17)—C(18)	2.24	−21.75	0.17	2.11	−20.59	0.22	0.13	1.16	0.05
B(3)—B(4)	0.85	−2.59	3.06	0.80	−2.70	4.27	0.05	0.10	1.21
B(3)—B(7)	0.79	−1.97	4.44	0.79	−2.42	5.66	0.00	0.46	1.22
B(3)—B(8)	0.86	−2.84	2.49	0.83	−3.39	3.73	0.03	0.55	1.24
B(4)—B(5)	0.81	−2.16	3.84	0.78	−2.40	5.31	0.02	0.23	1.47
B(4)—B(8)	0.82	−2.17	3.77	0.81	−2.86	4.60	0.02	0.69	0.83
B(4)—B(9)	0.79	−2.26	3.72	0.81	−3.03	3.90	0.02	0.77	0.18
B(5)—B(6)	0.83	−2.71	2.46	0.80	−2.67	4.31	0.03	−0.03	1.85
B(5)—B(9)	0.83	−2.41	2.55	0.81	−2.99	3.97	0.02	0.57	1.42
B(5)—B(10)	0.81	−2.19	3.27	0.80	−2.79	4.72	0.00	0.61	1.45
B(6)—B(10)	0.83	−1.93	3.81	0.83	−3.46	3.58	0.00	1.54	0.23
B(6)—B(11)	0.84	−2.23	4.69	0.79	−2.49	5.35	0.04	0.26	0.66
B(7)—B(8)	0.80	−2.13	3.29	0.81	−2.98	4.02	0.01	0.85	0.73
B(7)—B(11)	0.77	−1.47	6.04	0.78	−2.33	5.47	0.01	0.86	0.57
B(7)—B(12)	0.82	−2.70	2.38	0.81	−3.01	3.91	0.01	0.32	1.53
B(8)—B(9)	0.82	−2.34	2.24	0.78	−2.55	4.53	0.03	0.21	2.29
B(8)—B(12)	0.76	−1.46	7.29	0.78	−2.53	4.70	0.03	1.08	2.59
B(9)—B(10)	0.76	−1.38	5.56	0.79	−2.61	4.35	0.03	1.22	1.21
B(9)—B(12)	0.82	−2.28	2.63	0.79	−2.76	3.79	0.02	0.48	1.16
B(10)—B(11)	0.84	−2.45	2.82	0.81	−2.91	4.31	0.03	0.47	1.49
B(10)—B(12)	0.82	−2.25	2.43	0.78	−2.54	4.65	0.04	0.29	2.22
B(11)—B(12)	0.81	−2.29	3.73	0.81	−3.01	3.87	0.00	0.73	0.14

[a] Absolute value of the difference between the experimental and calculated values.
[b] Bond ellipticity.

necting the carborane polyhedron atoms differ only slightly (on the average, by only 3.5%, see Table 2). For the C—C and C—H bonds in the phenyl ring the differences are somewhat larger (at most 11%).

Unlike the electron density distribution function $\rho(\mathbf{r})$, the values of the Laplacian of the electron density, $\nabla^2\rho(\mathbf{r})$, calculated at some (3,−1) critical points differ in both magnitude and sign. For instance, X-ray diffraction data show that all chemical bonds in the polyhedron correspond to the shared type of interatomic interactions, because the $\nabla^2\rho(\mathbf{r})$ values at the (3,−1) critical points are negative. However, quantum-chemical calculations gave positive values of the Laplacian of the electron density at the (3,−1) critical points of the C(1)—B(4), C(1)—B(5), C(2)—B(7), and C(2)—B(11) bonds where a boron atom is bonded to only one carbon atom. Also, taking into account negative values of the local energy density at the (3,−1) critical points of these bonds, they can be considered as corresponding to the intermediate type of chemical interactions.

It should be noted that the type of chemical bonding for B—C interatomic interactions in carborane is rather sensitive to minor changes in the geometry. For instance, earlier it was pointed out that rotation of the phenyl substituent leads to a change in the character of interatomic interaction for the C(2)—B(3) and C(2)—B(6) bonds from the shared to intermediate type.[9] Based on this, one can assume that the differences between the C—B bonds in the crystal and in isolated molecule are due to the crystal packing effects.

The $\nabla^2\rho(\mathbf{r})$ values for the C(1)—C(2) bond in carborane are also strongly different. In particular, the value of the Laplacian of the electron density in the crystal is nearly an order of magnitude lower than in isolated molecule (−0.58 *vs.* −4.34 $e \cdot Å^{-5}$, respectively), being in both cases negative. Therefore, in contrast to 8,9,10,12-tetrafluoro-*o*-carborane,[17] the C(1)—C(2) bond in carborane **1** corresponds to shared type of interactions.

Taking into account that the $\nabla^2\rho(\mathbf{r})$ value at the (3,−1) critical point of the C(1)—C(2) bond in the crystal **1** is close to zero, we can assume that minor distortions of the carborane structure due to the introduction of bulky substituents or stereoelectronic effects will cause changes in the type of the C—C interatomic interactions. Probably, a similar effect is observed in compound **2** and governs an appreciable elongation of the C(1)—C(2) bond in, *e.g.*, triazine-substituted derivatives of *o*-carboranes[24,25] and the formation of pseudo-*closo*-structures of some metallacarboranes.[26—29]

The ellipticity (ε) values for the bonds in the polyhedron vary over rather wide intervals, namely, 0.09—7.29 for the crystal and 0.06—5.35 for isolated molecule **1**. A high ε value indicates a deviation of $\rho(\mathbf{r})$ from cylindrical symmetry, being typical of the bonds with a π-component or of the "banana" bonds as is the case of, *e.g.*, cyclopropane.[14] For instance, the average ellipticities of C—C bonds in the phenyl ring are 0.21 (isolated molecule) and 0.18 (crystal), which reflects the contribution of the π-component of these bonds. The C(1)—C(2) bond ellipticity is much higher (0.98 for isolated molecule **1** and 0.83 for the crystal). As the torsion angle θ varies from 0 to 90° (rotation of the phenyl substituent), the C(1)—C(2) bond ellipticity is a linear function of the C(1)—C(2) bond length and increases from 0.79 to 0.96.[9]

Low C(1)—C(13) bond ellipticity (ε = 0.09) is in good agreement with a small degree of charge transfer from the phenyl π-system to the antibonding orbital of the carborane C—C bond.[9,11]

The boron—boron bonds are characterized by the highest ellipticity values, which is consistent with the banana type ascribed to these bonds. For instance, the (3,−1) critical point is shifted from the line connecting the atoms of the B(9)—B(12) bond by 0.06 Å (*cf.* 0.02 Å for the atoms involved in the C(1)—C(2) and C(2)—B(7) bonds).

Electron delocalization over the polyhedron is most pronounced when comparing the $\rho(\mathbf{r})$ values at the (3,+1) critical points of triangular faces and at the (3,−1) critical points at the icosahedron edges. The $\rho(\mathbf{r})$ values at the (3,+1) critical points of triangular faces weakly depend on the ring type and vary by at most 0.03 (crystal) and 0.06 $e \cdot Å^{-3}$ (isolated molecule). The average electron density at the (3,+1) critical point (0.75 $e \cdot Å^{-3}$) is only slightly lower than the average $\rho(\mathbf{r})$ value at the (3,−1) critical points (0.86 and 0.82 $e \cdot Å^{-3}$). For comparison, the $\rho(\mathbf{r})$ values at the (3,+1) critical point and at the (3,−1) critical points of C—C bonds in the phenyl ring in the crystal **1** are 0.14 and 2.24 $e \cdot Å^{-3}$, respectively.

It should be noted that although the $\rho(\mathbf{r})$ values at the (3,+1) critical points of triangular faces weakly depend on the type of the interacting atoms, the values and even the sign of the Laplacian of the electron density $\nabla^2\rho(\mathbf{r})$ at these critical points of the CCB rings differ from the corresponding characteristics of the BBC and BBB rings. The BBC rings are characterized by positive $\nabla^2\rho(\mathbf{r})$ values for both the crystal (1.10 $e \cdot Å^{-5}$) and isolated molecule (2.20 $e \cdot Å^{-5}$), while the values of the Laplacian of the electron density for the remaining triangular faces are negative (−0.7——0.3 $e \cdot Å^{-5}$ in the crystal and −1.27——0.7 $e \cdot Å^{-5}$ in isolated molecule). Different signs of the Laplacian of the electron density indicate that at nearly the same $\rho(\mathbf{r})$ value at the (3,+1) critical point the curvature, λ_1, of the $\rho(\mathbf{r})$ function along the normal to the BBB and BBC faces is much higher than the corresponding values in the plane of the face (λ_2 and λ_3 eigenvalues).

When considering the maps of the Laplacian of experimental electron density, one must point out a charge concentration in the space between pairs of nuclei and charge depletion at the centers of the CCB and CBB faces (Fig. 5). As to the BBB faces, a charge depletion at the

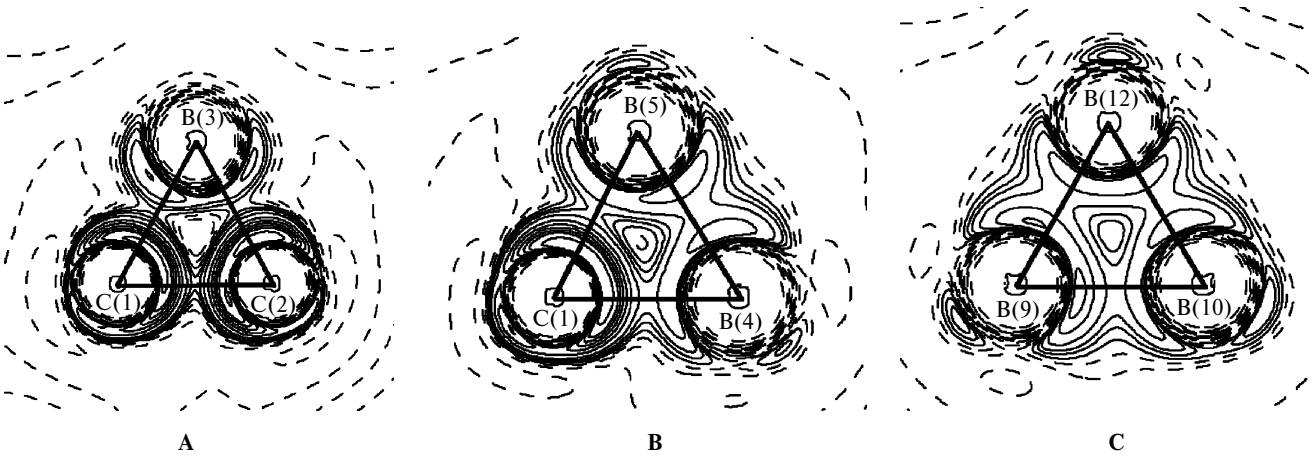

Fig. 5. Maps of distribution of the Laplacian of the electron density for the C(1)—C(2)—B(3) (**A**), C(1)—B(4)—B(5) (**B**), and B(9)—B(10)—B(12) (**C**) faces.

center is absent and the electron density is nearly uniformly distributed over the faces.

The most pronounced differences between the experimental and calculated electron density were found for the (3,+3) critical point at the center of the polyhedron. Namely, $\rho = 0.043$ e • Å^{-3} in the crystal and 0.105 e • Å^{-3} in isolated molecule **1** (*cf.* 0.17 e • Å^{-3} for compound **2**). The values of the Laplacian of the electron density at the (3,+3) critical point in the crystal and in isolated molecule **1** differ insignificantly (2.62 and 2.40 e • Å^{-5}, respectively).

The electron localization function. Recently, a dimensionless electron localization function (ELF) (η)[30] has been widely used in studies of electron density localization and delocalization in combination with the topological analysis. The ELF values show the extent to which the kinetic energy density at a given point of space differs from the corresponding value calculated using the Thomas—Fermi approximation for free electron gas. The η values exceeding 0.5 correspond to localization regions of the electron pairs and unpaired electrons. In this work the ELF values were calculated using the MORPHY program.[31]

In studies of polyhedral boron compounds the ELF method was applied to boranes only. It was shown[32] that the electron density is localized on triangular faces, which is consistent with the results of the topological analysis of the $\rho(\mathbf{r})$ function.

However, it was interesting to analyze the effect of the carbon atoms on the character of the ELF distribution in compound **1**. Until recently, the ELF distribution analysis was only possible for the calculated electron density, because the procedure requires determination of the local kinetic energy density, $g(\mathbf{r})$, calculated from the wave function. But the kinetic energy density necessary for the ELF calculations can be obtained from the gradient expansion.[33] Evaluation of different approximations showed that the best results are obtained using the Kirzhnitts scheme.[34]

By and large, this procedure for constructing the experimental ELF permits detection of the same structural features as those found for the theoretical ELF, although agreement between the experimental data and results of calculations in the region of covalent bonds is not always good. For instance, studies of urea,[33] tetraacetylethane,[35] diphenylphosphonic acid,[36] peri-substituted naphthalenes,[37] and a 3-borabicyclo[3.3.1]nonane derivative[38] revealed a double rather than single ELF maximum in the region of covalent bonds. This artifact is due to limitations of the approximations[34] used for the description of the regions with a high curvature of the $\rho(\mathbf{r})$ function.[33] However, in the case of weak intramolecular and intermolecular contacts[35,37,38] and in localization of the lone electron pairs[36] this approximation allows subtle electronic effects to be analyzed.

In this connection it was interesting to compare the experimental and calculated ELF distribution in molecule **1** and to assess the applicability of the procedure mentioned above to the analysis of the character of electron delocalization in polyhedral systems.

First, we will consider the theoretical ELF distribution maps (Fig. 6). On the C(1)—C(2)—B(3) face, a contour line of height 0.85 describes nearly the whole space between the three atoms, but peaks of height 0.9 between pairs of interacting atoms are clearly seen. This points to localization of electron pairs in these regions. Two peaks framed by the contour lines of height 0.9 on the C(1)—B(4)—B(5) face should be pointed out. One peak is between the boron atoms and the other is a highly diffuse peak corresponding to the interaction between the C atom and two adjacent boron atoms. On the B(8)—B(9)—B(12) face, the interatomic space is framed by a contour line of height 0.9, which is uniformly distributed over the face. Thus, in contrast to polyhedral bo-

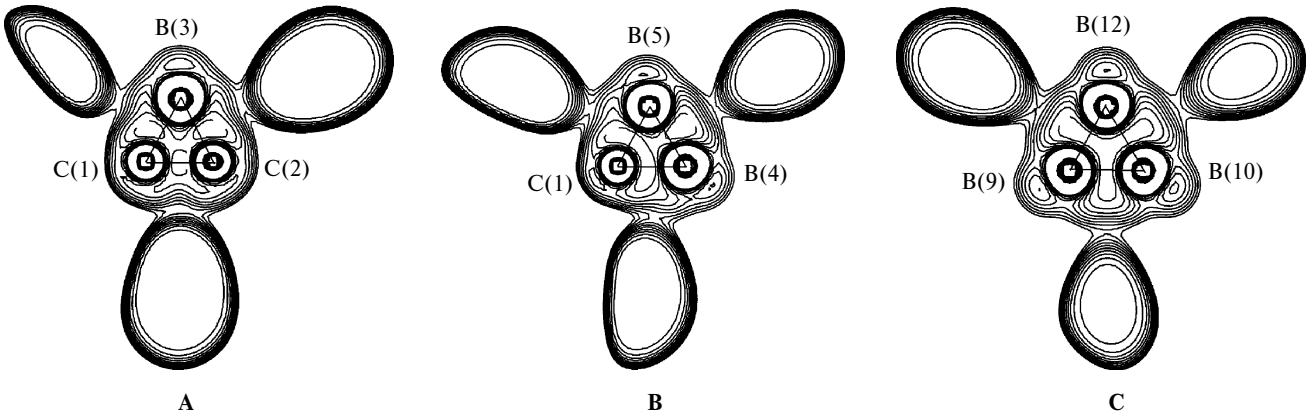

Fig. 6. Maps of theoretical ELF distribution over the C(1)—C(2)—B(3) (**A**), C(1)—B(4)—B(5) (**B**), and B(9)—B(10)—B(12) (**C**) faces.

ranes, in the systems under study the introduction of carbon atoms leads to a shift of the ELF maxima on the faces and to a change in the character of electron delocalization over the surface of the polyhedron.

It should be noted that qualitative analysis of the ELF distribution maps reveals the same trends as those established in the studies of the experimental and theoretical maps of the Laplacian of the electron density distribution and the DED distribution maps (see above).

However, the ELF function calculated from experimental data exhibits no features of the electron distribution over triangular faces (see above). As can be seen in the all three cross-sections (Fig. 7), the ELF distribution obeys a qualitatively identical pattern. The ELF maxima were found near atoms, whereas at the centers of the faces and at the edges of the polyhedron the η value is at most 0.65.

Thus, the ELF function calculated from experimental data in the framework of the model proposed[33] seems to be inapplicable to the analysis of delocalized systems.

Intra- and intermolecular contacts H...H

High accuracy of the $\rho(\mathbf{r})$ function we obtained allows us to hope that it will be useful for the analysis of not only strong chemical bonds but also intermolecular contacts.

As mentioned above, analysis of the critical points in the regions of the intramolecular H...H contacts allowed us to localize the (3,−1) critical points between the same pairs of atoms, H(2)...H(18) and H(5)...H(14), as in the calculations. The topological characteristics of these contacts in the crystal are in good agreement with the results of calculations (Table 3).

In contrast to the triangular carborane faces, here good agreement was obtained for not only the $\rho(\mathbf{r})$ and $\nabla^2\rho(\mathbf{r})$ values but also for the kinetic and potential energy densities calculated in the approximation[34] mentioned above. These H...H contacts are characterized by large positive values of $\nabla^2\rho(\mathbf{r})$ and of the electronic energy density and correspond to closed-shell interactions in contrast to the B—C bonds considered above.

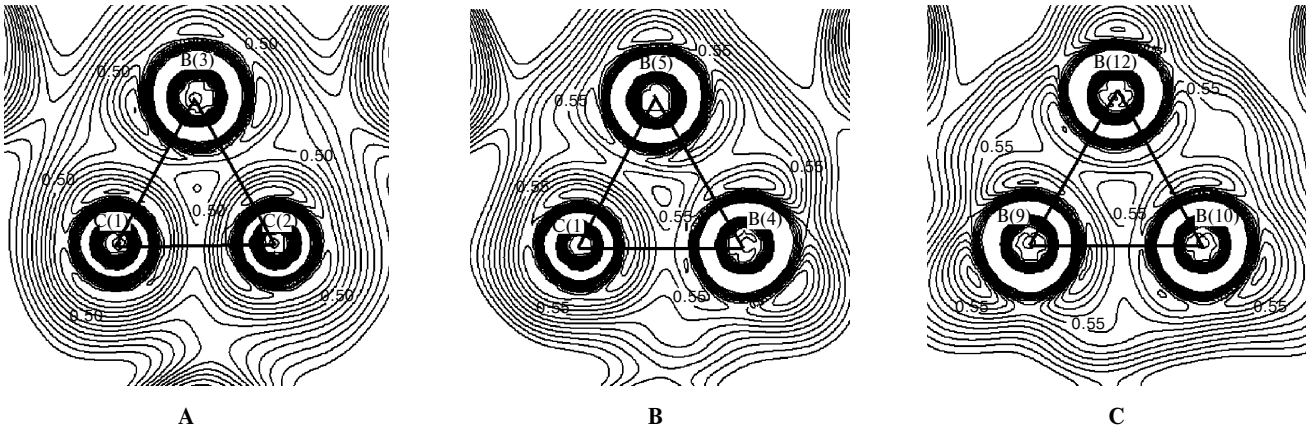

Fig. 7. Maps of experimental ELF distribution over the C(1)—C(2)—B(3) (**A**), C(1)—B(4)—B(5) (**B**), and B(9)—B(10)—B(12) (**C**) faces.

Table 3. Geometric and topological parameters of intramolecular H...H contacts in the crystal according to X-ray diffraction data and in isolated molecule (obtained from B3LYP/6-311G** calculations)

Contact	Crystal				Isolated molecule			
	$d_{H...H}$/Å	$\rho(\mathbf{r})$/e·Å^{-3}	$\nabla^2\rho(\mathbf{r})$/e·Å^{-5}	ε^a	$d_{H...H}$/Å	$\rho(\mathbf{r})$/e·Å^{-3}	$\nabla^2\rho(\mathbf{r})$/e·Å^{-5}	ε^a
C(2)—H(2)...H(18)—C(18)	2.041 2.087[b]	0.082	1.081	0.47	2.077	0.073	1.003	0.610
C(5)—H(5)...H(14)—C(14)	2.148 2.093[b]	0.083	0.886	0.08	2.173	0.069	0.845	0.548

[a] Bond ellipticity.
[b] Obtained from quantum-chemical calculations of crystal **1**.

Recently,[39] it was established that these H...H interactions can cause an additional stabilization of molecules. The energy of these contacts estimated from the potential energy density[40] lies between 1.8 and 2.2 kcal mol^{-1}, being similar to the energy of weak C—H...O interactions.

Analysis of the data on the X—H...H—X (X = B, C) intermolecular contacts in the crystals of organic carborane derivatives, retrieved from the CSD revealed that the H...H distances lie in a wide range beginning with 2.0 Å and having no exact upper bound (this is characteristic of all intermolecular contacts) and that the X—H...H angles lie between 100° and 170°. The characteristics of the intermolecular contacts obtained for compound **1** lie within these intervals (see Table 1); however, the range of distances at which the intermolecular contacts in question do occur must be determine more accurately.

In this connection a convenient way is to search for the (3,−1) critical points in the region of the intermolecular H...H contacts mentioned above. Similarly to the analysis of intramolecular contacts, we found the (3,−1) critical points between pairs of atoms separated by distances that are shorter or slightly longer than the sum of the Van der Waals radii of two hydrogen atoms. The topological characteristics of the intermolecular H...H contacts are listed in Table 4. These contacts correspond to closed-shell interactions, being longer and consequently weaker than the intramolecular contacts. The $\sigma(\mathbf{r})$ values for the intermolecular contacts are on the average four times lower and the interaction energies calculated in the same approximation[40] are at most 1 kcal mol^{-1} (see Table 4). The X—H...H and H...H—X (X = C_{carb}, C_{phenyl}, B) angles lie in the range 125—142°, being somewhat larger than in the case of intramolecular contacts.

Of course, account must be taken of the fact that from the standpoint of crystal chemistry there is no contact between two hydrogen atoms separated by more than 2.4 Å; however, our procedure allows the range of distances for this type of interactions to be extended.

In order to estimate the contribution of the intermolecular contacts mentioned above to the energy of the crystal lattice, we performed DFT calculations of the crystal structure of compound **1** using the CPMD program.[41] The energy of the crystal lattice determined from the results of calculations (see Experimental) is 65.5 kcal mol^{-1}. Thus, the energy per molecule in the unit

Table 4. Topological parameters of H...H intermolecular contacts in the crystal of compound **1** according to X-ray diffraction data

Contact*	$\rho(\mathbf{r})$/e·Å^{-3}	$\nabla^2\rho(\mathbf{r})$/e·Å^{-5}	ε	$g(r)$	$V(r)$	$h_e(\mathbf{r})$	E_{cont}/kcal mol^{-1}
C(2)—H(2)...H(7′)—B(7′)	0.041	0.55	0.057	0.0044	−0.003	0.0013	0.94
C(2)—H(2)...H(12′)—B(12′)	0.032	0.4	0.762	0.0032	−0.0022	0.001	0.69
B(3)—H(3)...H(11′)—B(11′)	0.023	0.28	0.229	0.0022	−0.0014	0.0007	0.44
B(3)—H(3)...H(17′)—C(17′)	0.03	0.38	0.068	0.003	−0.002	0.001	0.63
B(4)—H(4)...H(10′)—B(10′)	0.029	0.39	0.151	0.003	−0.002	0.001	0.63
B(5)—H(5)...H(10′)—B(10′)	0.021	0.42	0.723	0.0031	−0.0018	0.0013	0.56
B(6)—H(6)...H(15′)—C(15′)	0.029	0.39	0.143	0.003	−0.002	0.001	0.63
B(7)—H(7)...H(12′)—B(12′)	0.041	0.44	0.079	0.0036	−0.0027	0.0009	0.85
B(8)—H(8)...H(11′)—B(11′)	0.032	0.37	0.187	0.003	−0.0021	0.0009	0.66
B(9)—H(9)...H(14′)—C(14′)	0.036	0.45	0.076	0.0036	−0.0025	0.0011	0.78
B(9)—H(9)...H(15′)—C(15′)	0.027	0.41	0.16	0.0031	−0.002	0.0011	0.63
B(10)—H(10)...H(10′)—B(10′)	0.039	0.36	0.336	0.003	−0.0023	0.0007	0.72
B(12)—H(12)...H(17′)—C(17′)	0.031	0.42	0.033	0.0033	−0.0022	0.0011	0.69

* Primed atoms were generated by the symmetry transformations (see note[a] to Table 1).

cell is 16.4 kcal mol^{-1}, which falls in the range of values of the sublimation energies of organic compounds.[42]

The total energy of contacts per molecule in the unit cell calculated from experimental data using the procedure mentioned above is 17.0 kcal mol^{-1}. It seems likely that the energy of the crystal lattice is nearly completely determined by the structure-forming intermolecular H...H contacts. Overestimation of the experimental energy per molecule in the crystal lattice seems to be due to small differences between the experimental and calculated lengths of intermolecular contacts.

The calculated and experimental geometry of molecule **1** in the crystal differ only slightly. For instance, the C(2)—C(1)—C(13)—C(18) torsion angle responsible for the conformation of the phenyl substituent increases from 18.7 to 20.4° and the C(1)—C(2) bond is shortened from 1.645 to 1.643 Å. Changes in the system of X—H...H—X (X = C, B) intermolecular contacts are more pronounced. In particular, the number of the neighboring molecules involved in the formation of H...H contacts in the calculated crystal structure decreased by a value of three compared to the experiment. According to calculations, each molecule forms a total of 16 contacts (*cf.* a total of twenty-five contacts found in the experiment); the geometric parameters of the contacts found in the calculations are also somewhat changed (see Table 1).

An explanation for these features is provided by underestimation of these electron correlation effects in the DFT calculations. Usually, this is insignificant for calculations of isolated molecules but leads to deviation from experimental data in the presence of weak interactions.

Although the H...H intermolecular contacts are much weaker than intramolecular contacts, they play the key role in the formation of the crystal packing in the compounds structurally similar to **1**. If the *ortho*-carborane molecule contains only one substituent at a carbon atom, intermolecular interactions cannot always provide a rigid icosahedron geometry (especially in the case of room-temperature X-ray diffraction experiments). Often, this is the reason for disorder of corresponding the carbon atom, which precludes its localization in, *e.g.*, one crystallographically independent molecule of the α-**1** polymorph.

Thus, comparison of the theoretical and experimental electron density distributions (σ(**r**) functions) shows that modern X-ray diffraction methods are suitable for investigations of the peculiarities of electron delocalization in carboranes and of the nature of weak intra- and intermolecular H...H contacts and even for estimation of their energies. The last-mentioned possibility is particularly attractive for studies of polymorphism, because this permits a direct evaluation of the stability of different polymorphs from experimental data. Most topological characteristics of the electron density distribution are not only in qualitative but also in quantitative agreement with the results of calculations.

Experimental and Calculation Procedure

X-ray diffraction study of compound **1** ($C_8H_{16}B_{10}$) was carried out on a Smart CCD 1000K automated three-circle diffractometer (Mo-Kα radiation, graphite monochromator, ω-scan technique, $2\theta_{max} \leq 95°$) at $T = 110$ K. At this temperature, the crystals are monoclinic: $a = 6.979(1)$, $b = 8.388(1)$, $c = 21.728(3)$ Å, $\beta = 97.978(1)°$, $V = 1259.7(3)$ Å^3, $d_{calc} = 1.162$ g cm^{-3}, M = 220.31, $F(000) = 456$, $\mu = 0.53$ cm^{-1}, $Z = 4$ ($Z' = 1$), and the space group is $P2_1/c$. Out of 33170 measured reflections, a total of 10866 independent reflections were included in the calculations and structure refinement ($R_{int} = 0.0253$). The absorption correction was included semi-empirically using the equivalent reflection and the SADABS program.[43] The structure was solved by the direct method and refined using the full-matrix least-squares method in the full-matrix anisotropic approximation based on F^2_{hkl}. Hydrogen atoms were located from the difference electron density Fourier syntheses and included in the refinement isotropically. The final reliability factors were as follows: $R = 0.0435$ based on a total of 7405 reflections with $I > 2\sigma(I)$, $wR_2 = 0.0922$, and GOOF = 1.070 based on all reflections. All calculations were carried out using the SHELXTL PLUS software.[44]

To obtain the analytical form of the experimental electron density distribution function, a multipole refinement of the X-ray diffraction data was performed in the framework of the Hansen—Coppens model[45] using the XD program complex.[46] The multipole refinement of all non-hydrogen atoms included refinement of the coordinates, anisotropic thermal parameters, and multipole parameters up to the octupole level ($l = 3$) based on F_{hkl}. The multipole refinement parameters of the phenyl ring carbon atoms were refined taking into account the local symmetry m.[47] Positions of hydrogen atoms and their isotropic thermal parameters were not refined. Before the refinement, the C—H and B—H distances were normalized to the "ideal" values (1.08 and 1.20 Å, respectively) obtained from quantum-chemical calculations. The hydrogen atoms were refined up to the dipole level ($l = 2$) with inclusion of cylindrical symmetry. Correctness of the calculated anisotropic parameters of atomic displacements was estimated using Hirshfeld´s test,[48] which for chemical bonds was at most $9 \cdot 10^{-4}$ Å^2. The multipole refinement converged to $R = 0.028$, $wR = 0.025$, and GOOF = 1.53 based on 6807 reflections with $I > 3\sigma(I)$. The electron density maxima in the residual density maps, $(\rho(\mathbf{r})_{exp} - \rho(\mathbf{r})_{multip})$, were no higher than 0.11 e·Å^{-3}. The ELF values were calculated from the X-ray diffraction data using the WINXPRO program.[49,50]

Quantum-chemical calculations of 1-phenyl-*o*-carborane were carried out using the GAUSSIAN-98 suite of programs[51] with the B3LYP functional[52] and the 6-311G(d,p) basis set. Geometry optimization of the molecule with C_1 symmetry was performed with a preset torsion angle θ value of 18.7° and full optimization of the remaining geometric parameters using the results of the X-ray diffraction study as a starting geometry. Standard error values of $4.5 \cdot 10^{-4}$ and $1.8 \cdot 10^{-3}$ rel. u. for the maximum strength and displacement, respectively, were taken as the convergence criteria. The topological analysis of the σ(**r**) function was performed using the MORPHY-98 program[31] and the wave function obtained from the B3LYP calculations.

Crystal structure calculations with full geometry optimization at preset unit cell parameters were carried out using the CPMD program[32] with the PBE exchange-correlation func-

tional[53] and a plane wave basis set (kinetic energy ≤ 25 Ry). A part of the wave function corresponding to the core electrons was described using the Vanderbilt pseudopotentials.[54] Calculations of crystal **1** were performed with periodic boundary conditions and inclusion of only the Γ-points in the Brillouin zone using the experimental unit cell parameters. The energy and structural parameters of isolated molecule **1** were obtained from calculations for a cubic cell with a 15 Å edge. Since plane waves are delocalized in space, the results of calculations are free from the basis set superposition error.

The authors express their gratitude to S. P. Knyazev (Moscow State Academy of Fine Chemical Technology) for kindly submitting a single crystal of 1-phenyl-*o*-carborane. This work was carried out with the financial support from the Russian Foundation for Basic Research (Project Nos 03-03-32214 and 02-07-90169), the Russian Federation Presidential Foundation (Programs for support of the Leading Scientific Schools (grant NSh 1060.2003.30), and the young Ph.D. researchers (MK-1209.2003.03)).

References

1. K. A. Lyssenko and M. Yu. Antipin, *Izv. Akad. Nauk. Ser. Khim.*, 2004, 11 [*Russ. Chem. Bull., Int. Ed.*, 2004, **53**, 10].
2. M. J. Hardie and C. L. Raston, *Eur. J. Inorg. Chem.*, 1999, 195.
3. M. J. Hardie, C. L. Raston, and B. Wells, *Chem. Eur. J.*, 2000, **6**, 3293.
4. P. C. Andrews, M. J. Hardie, and C. L. Raston, *Coord. Chem. Rev.*, 1999, **189**, 169.
5. P. D. Godfrey, W. J. Grigsby, P. J. Nichols, and C. L. Raston, *J. Am. Chem. Soc.*, 1997, **119**, 9283.
6. H. Lee, C. B. Knobler, and M. F. Hawthorne, *Chem. Commun.*, 2000, 2485.
7. L. A. Leites, *Chem. Rev.*, 1992, **92**, 279.
8. P. T. Brain, J. Cowie, D. J. Donohoe, D. Hnyk, D. W. H. Rankin, D. Reed, B. D. Red, H. E. Robetson, A. J. Welch, M. Hofmann, and P. Schleyer, *Inorg. Chem.*, 1996, **35**, 1701.
9. I. V. Glukhov, M. Yu. Antipin, and K. A. Lyssenko, *Eur. J. Inorg. Chem.*, 2004, **7**, 1379.
10. E. S. Alekseyeva, M. A. Fox, J. A. K. Howard, J. A. H. MacBride, and K. Wade, *Appl. Organomet. Chem.*, 2003, **17**, 499.
11. M. Tsuji, *J. Org. Chem.*, 2004, **69**, 4063.
12. R. L. Thomas, G. M. Rosiar, and A. J. Welch, *Acta Crystallogr.*, 1996, **C52**, 1024.
13. *Cambridge Crystallographic Database*, release 2003.
14. R. F. W. Bader, *Atoms in Molecules. A Quantum Theory*, Clarendron Press, Oxford, 1990.
15. R. F. W. Bader, *J. Chem. Phys.*, 1998, **A102**, 7314.
16. M. Yu. Antipin, A. V. Polyakov, V. G. Tsirel´son, M. Kapkhan, V. V. Grushin, and Yu. T. Struchkov, *Metalloorg. Khim.*, 1990, **3**, 421 [*Organomet. Chem. USSR*, 1990, **3**, 421].
17. K. A. Lyssenko, M. Y. Antipin, and V. N. Lebedev, *Inorg. Chem.*, 1998, **37**, 5834.
18. R. F. W. Bader and D. A. Legarre, *Can. J. Chem.*, 1992, **70**, 657.
19. M. Yu. Antipin, R. Boese, D. Blaeser, and A. Maulitz, *J. Am. Chem. Soc.*, 1997, **119**, 326.
20. P. Macchi and A. Sironi, *Coord. Chem. Rev.*, 2003, **238—239**, 383.
21. K. A. Lysenko, M. Yu. Antipin, and V. N. Khrustalev, *Izv. Akad. Nauk. Ser. Khim.*, 2001, 1465 [*Russ. Chem. Bull., Int. Ed.*, 2001, **50**, 1529].
22. A. J. Welch, *Steric Effects in Metallacarboranes Metal Clusters in Chemistry*, Eds P. Braunstein, L. A. Oro, and P. R. Raithby, Wiley-VCH, 1999, 69.
23. J. Llop, C. Viñas, F. Teixidor, L. Victori, R. Kivekäs, and R. Sillanpää, *Organometallics*, 2001, **20**, 4024.
24. O. N. Chupakhin, A. M. Prokhorov, D. N. Kozhevnikov, V. L. Rusinov, I. V. Glukhov, Z. A. Starikova, V. A. Ol´shevskaya, V. N. Kalinin, and M. Yu. Antipin, *Izv. Akad. Nauk. Ser. Khim.*, 2004, 1175 [*Russ. Chem. Bull., Int. Ed.*, 2004, **53**, 1223].
25. O. N. Chupakhin, A. M. Prokhorov, D. N. Kozhevnikov, V. L. Rusinov, V. N. Kalinin, V. A. Olshevskaya, I. V. Glukhov, and M. Yu. Antipin, *Mendeleev Commun.*, 2003, **4**, 165.
26. N. Carr, D. F. Mullica, E. L. Sappenfield, and F. G. A. Stone, *Organometallics*, 1992, **11**, 3697.
27. P. T. Brain, M. Bühl, J. Cowie, Z. G. Lewis, and A. J. Welch, *J. Chem. Soc., Dalton Trans.*, 1996, 231.
28. J. Kim, M. Lamrani, J. Hwang, and Y. Do, *Chem. Commun.*, 1997, 1761.
29. F. Teixidor, M. A. Flores, C. Vinas, R. Sillanpaa, and R. Kivekas, *J. Am. Chem. Soc.*, 2000, **122**, 1963.
30. A. Savin, R. Nesper, S. Wengert, and T. Fassler, *Angew. Chem., Int. Ed. Engl.*, 1997, **36**, 1809.
31. a) *MORPHY98, a Topological Analysis Program Written by P. L. A. Popelier with a Contribution from R. G. A. Bone (UMIST, Engl, EU)*; b) P. Popelier, *Chem. Phys. Lett.*, 1994, **228**, 160.
32. H. Binder, R. Kellner, K. Vaas, M. Hein, F. Baumann, M. Wanner, W. Kaim, U. Wedig, W. Honle, H. G. von Schnering, O. Groeger, and G. Engelhardt, *Z. Anorg. Allg. Chem.*, 1999, **625**, 1638.
33. V. Tsirelson and A. Stash, *Chem. Phys. Lett.*, 2002, **351**, 142.
34. D. A. Kirzhnitts, *Zh. Eksp. Teor. Fiz.*, 1957, **5**, 64 [*Sov. J. Exp. Theor. Phys.*, 1957, **5**, 64 (Engl. Transl.)].
35. K. A. Lyssenko, D. V. Lyubetsky, and M. Yu. Antipin, *Mendeleev Commun.*, 2003, 60.
36. K. A. Lyssenko, G. V. Grintselev-Knyazev, and M. Yu. Antipin, *Mendeleev Commun.*, 2002, 128.
37. K. A. Lyssenko, S. M. Aldoshin, and M. Yu. Antipin, *Mendeleev Commun.*, 2004, 98.
38. K. A. Lyssenko, M. Yu. Antipin, M. E. Gurskii, Yu. N. Bubnov, A. L. Karionova, and R. Boese, *Chem. Phys. Lett.*, 2004, **384**, 40.
39. C. F. Matta, J. Hernández, T. Tang, and R. Bader, *Chem. Eur. J.*, 2003, 1940.
40. E. Espinosa, E. Mollins, and C. Lecomte, *Chem. Phys. Lett.*, 1998, **285**, 170.
41. J. Hutter, P. Ballone, M. Bernasconi, P. Focher, E. Fois, S. Goedecker, M. Parrinello, and M. Tuckerman (1995–2001) CPMD v. 3.7.2, MPI für Festkorperforschung and IBM Zürich Research Laboratory.
42. J. Bernstein, *Polymorphism in Molecular Crystals*, Clarendon Press, Oxford, 2002.

43. G. M. Sheldrick, *SADABS*, 1997, Bruker AXS Inc., Madison, WI-53719, USA.
44. G. M. Sheldrick, *SHELXTL-97*, Version 5.10, Bruker AXS Inc., Madison, WI-53719, USA.
45. N. K. Hansen and P. Coppens, *Acta Crystallogr.*, 1978, **A34**, 909.
46. T. Koritsanszky, S. T. Howard, T. Richter, P. Macchi, A. Volkov, C. Gatti, P. R. Mallinson, L. J. Farrugia, Z. Su, and N. K. Hansen, *XD - A Computer Program Package for Multipole Refinement and Topological Analysis of Charge Densities from Diffraction Data*, 2003.
47. K. Kurki-Suonio, *Isr. J. Chem.*, 1977, **16**, 115.
48. F. L. Hirshfeld, *Acta Crystallogr.*, 1976, **A32**, 239.
49. A. Stash and V. Tsirelson, *J. Appl. Crystallogr.*, 2002, **35**, 371.
50. A. Stash and V. Tsirelson, *WinXPRO — a Program for Calculation of the Crystal and Molecular Properties Using the Model Electron Density*, Moscow (Russia), 2001. Further information is available at URL http://xray.nifhi.ru/wxp/
51. M. J. Frisch, G. W. Trucks, H. B. Schlegel, G. E. Scuseria, M. A. Robb, J. R. Cheeseman, V. G. Zakrzewski, J. A. Montgomery, Jr., R. E. Stratmann, J. C. Burant, S. Dapprich, J. M. Millam, A. D. Daniels, K. N. Kudin, M. C. Strain, O. Farkas, J. Tomasi, V. Barone, M. Cossi, R. Cammi, B. Mennucci, C. Pomelli, C. Adamo, S. Clifford, J. Ochterski, G. A. Petersson, P. Y. Ayala, Q. Cui, K. Morokuma, D. K. Malick, A. D. Rabuck, K. Raghavachari, J. B. Foresman, J. Cioslowski, J. V. Ortiz, A. G. Baboul, B. B. Stefanov, G. Liu, A. Liashenko, P. Piskorz, I. Komaromi, R. Gomperts, R. L. Martin, D. J. Fox, T. Keith, M. A. Al-Laham, C. Y. Peng, A. Nanayakkara, M. Challacombe, P. M. W. Gill, B. Johnson, W. Chen, M. W. Wong, J. L. Andres, C. Gonzalez, M. Head-Gordon, E. S. Replogle, and J. A. Pople, *Gaussian 98*, *Revision A.7*, Gaussian, Inc., Pittsburgh (PA), 1998
52. A. D. Becke, *J. Chem. Phys.*, 1993, **98**, 5648.
53. J. P. Perdew, K. Burke, and M. Ernzerhof, *Phys. Rev. Lett.*, 1996, **77**, 3865.
54. D. Vanderbilt, *Phys. Rev.*, 1985, **B41**, 7892.

Received June 23, 2004